Geophys. J. R. astr. Soc. (1974) **36**, 377–398.

The Tau Method for Inversion of Travel Times—I. Deep Seismic Sounding Data

E. N. Bessonova, V. M. Fishman, V. Z. Ryaboyi and G. A. Sitnikova

(Received 1973 June 20)*

Summary

A new method for solving the inverse problem of seismology is described in this paper. The problem is formulated as follows: the travel times of body waves are given at a discrete set of points, and we are required to find in the (V, Y) plane (V being the velocity and Y the depth) the closed area which contains all velocity-depth curves corresponding to the given data. The method is based on the use of the function $\tau(p) = T(p) - pX(p)$, p being the ray parameter, T the travel time, and X the epicentral distance. This method has the following advantages: it does not necessarily involve the estimation of p by numerical differentiation of the travel times; and it does not involve any interpolation of the travel-time curve between actual observations. Only two assumptions are made: spherical symmetry of the structure (the absence of horizontal inhomogeneities), and the postulation of a lower limit for the velocity in low velocity zones. The function $\tau(p)$ is estimated directly from the observed (T_i, X_i) as a singular solution of the Clairaut equation with free term $T(X)$.

Application of the method is illustrated using data from deep seismic sounding in Turkmenistan.

1. Introduction

This paper deals with determination of the limits for velocity-depth curves from discrete travel-time data of refracted and reflected body waves. We assume the medium to be horizontally homogeneous, so that the velocity depends only upon the distance from the centre of the Earth; the wave propagation is assumed to follow from ray theory.

This problem has been investigated by Gerver & Markushevitch (1966) for the general case in which low velocity zones may be present. The exact mathematical formulation of the problem is as follows.

Waves are radiated from a point at the surface of a sphere of radius R; they propagate along rays determined by the equation:

$$p = rv^{-1}(r) \sin \gamma(r)$$

where r is the radial co-ordinate, $v(r)$ is the velocity of wave propagation at radius

* Received in original form 1973 January 5

r; $\gamma(r)$ is the angle between the radius vector and the ray, and p is the ray parameter. Then the parametric equations of the travel-time curve are:

$$t(p) = 2 \int_{r(p)}^{R} r v^{-2}(r)[r^2 v^{-2}(r) - p^2]^{-\frac{1}{2}} \, dr$$

$$\Delta(p) = 2p \int_{r(p)}^{R} r^{-1}[r^2 v^{-2}(r) - p^2]^{-\frac{1}{2}} \, dr$$

$$p = dt/d\Delta.$$

The problem is to determine $v(r)$ from $t(\Delta)$. It is possible (Gerver & Markushevitch 1966) to reduce this problem to the analogous one for a half-plane $Y \geqslant 0$ by the transformation:

$$X = R\Delta/v(R) \qquad Y = Rv^{-1}(r) \ln (R/r)$$

$$V(Y) = \frac{v\{R \exp[-v(R)\, Y/R]\}}{v(R) \exp[-v(R)\, Y/R]} .$$

After this transformation we have:

$$\left.\begin{aligned} X(p) &= \int_0^{Y(p)} p[u^2(y) - p^2]^{-\frac{1}{2}} \, dy \\ T(p) &= \int_0^{Y(p)} u^2(y)[u^2(y) - p^2]^{-\frac{1}{2}} \, dy \end{aligned}\right\} \tag{1}$$

where $u(y) = V^{-1}(y)$ is wave slowness (reciprocal velocity); $2X(p)$ is epicentral distance; and $2T(p)$ is the arrival time along a ray with parameter p.

We assume, as in Gerver & Markushevitch (1966), that the function $V(y)$ is piecewise continuous along with its first derivative and has a finite number of low velocity zones. The low velocity zone with index i begins at the depth $\bar{y}_i$ where $u(y_i) = q_i$, and ends at the depth $\dot{y}_i$, so that

$$u(y) > q_i \quad \text{if} \quad \bar{y}_i < y < \dot{y}_i.$$

Then the solution of the inverse problem is given by:

$$Y(p) = 2\pi^{-1} \int_p^1 X(q)[q^2 - p^2]^{-\frac{1}{2}} \, dq + \sum_i 2\pi^{-1} \int_{\bar{y}_i}^{\dot{y}_i} \tan^{-1}\{[u^2(y) - q_i^2]/[q_i^2 - p^2]\}^{\frac{1}{2}} \, dy. \tag{2}$$

The first term is the Herglotz–Wiechert integral. In the second term the summation is taken over all low velocity zones with $q_i > p$. Equation (2) specifies an area containing all velocity-depth curves consistent with the given travel time (Gerver & Markushevitch 1966).

To use equation (2) it is necessary to know the exact travel times for all distances X. In practice, however, we know only a discrete number of travel-time data, and these data contain some errors. Thus most existing methods of inversion require an interpolation of the travel-time curve between the given data points.

For instance, Knopoff & Teng (1965) approximate the travel-time curve by several functions of varying complexity. The most general method, trial and error, does not require interpolation of data (Yanovskaya 1962; Yanovskaya & Asbel 1964; Lehmann 1962; Valus 1968). However, this method has its own disadvantages; it needs *a priori* specification of the type of function by which $V(r)$ is represented, and of the limits for this function; these limits can be supplied by our method.

Backus & Gilbert (1970) suggested an inversion method using discrete travel-time data; they treat the given data set as a linear functional on the space of velocity-depth profiles. But the travel time is a non-linear functional, so in this method one looks only for the velocity-depth curves that are near some given curve, but we cannot find out by this method if there exist any other velocity-depth curves which are different from the given one and yet are in good agreement with the given travel times.

In previously reported work (Bessonova, Fishman & Sitnikova, 1970; see also Keilis-Borok 1971) we had suggested an algorithm for constructing the envelope of all possible velocity-depth models that are consistent with a finite number of data. The data required were travel times, distances, and ray parameters. We had not interpolated the travel-time curve, and had not accepted any subjective hypotheses about the velocity-depth curve, but we did assume that the data are exact (i.e. contain no errors); this assumption involves some difficulties in practical applications.

In this paper we consider the case when the travel-time data are determined at a discrete number of distances (with errors in both distance and time). Values of the ray parameter are not required, and we need not calculate them by numerical differentiation of the travel-time curve. The only subjective hypothesis we make is that the velocity in the low velocity zones is greater than some given constant. In the present paper we apply the 'τ method' to deep seismic sounding data in order to investigate the velocity distribution in the Earth's crust. In a subsequent paper we will use earthquake data to investigate the velocity distribution in the mantle.

This paper is based on theoretical results of Gerver & Markushevitch (1966, 1967). In the 1966 paper they introduced the function $\tau(p)$:

$$\tau(p) = T(p) - pX(p) = \int_0^{Y(p)} [u^2(y) - p^2]^{\frac{1}{2}}\, dy.$$

This function holds a prominent place in our method; it connects travel times and velocity-depth curves; the title of the present paper was chosen to reflect the basic role of the function $\tau(p)$.

Several papers relevant to our present work have appeared recently. McMechan & Wiggins (1972) and Wiggins, McMechan & Toksöz (1973) expanded our 'method of parallelograms' (Bessonova *et al.* 1970) for the interpretation of real data. With their approach, it is necessary to derive narrow limits for the function $X(p)$ from observed data (p_i, X_i), which is a very subjective matter. We know that the error in the value of a function is proportional to the error in the argument and to the derivative of the function. With seismic data, the derivative $X'(p)$ can be very large, and the values of p calculated by differentiation of the travel-time curve (or known from array measurements) contain large uncertainties.

In comparison with this, in our method we estimate $\tau(p)$ for a given value of p as the extreme value of some function. Since the derivative at an extremum is zero, this is easy. Our method is stable to errors in the data, in the sense that the uncertainty in $\tau(p)$ is of the same order as the uncertainty in $T_i(X_i)$, and the limits for the velocity-depth curve can be derived by integrating the limits for $\tau(p)$ with a weighting function. Further comments on the McMechan & Wiggins paper will be made in our subsequent paper, where we use the same data as they.

Johnson & Gilbert (1972a, b) also used the function $\tau(p)$, but their method of calculation of $\tau(p)$ has practical difficulties. First, it is necessary to know the value of the ray parameter p; then $X(p)$ is calculated as the average value of $X_i(p_i)$ for p_i in some interval. As will be shown below, the result of such a calculation is often incorrect because of errors in p_i. Moreover, the calculation of $\tau(p)$ by integrating $X(p)$ is incorrect, since in the presence of low-velocity zones we have

$$\tau(p) = \int_p^1 X(q)\,dq + \Sigma\sigma_i.$$

In the present paper, the function $\tau(p)$ is estimated directly from $T_i(X_i)$ without using the ray parameter values.

2. Properties of $\tau(p)$

The function $\tau(p)$ is connected with the velocity-depth curve by the equation

$$\tau(p) = \int_0^{Y(p)} [u^2(y)-p^2]^{\frac{1}{2}}\,dy \tag{3}$$

(Gerver & Markushevitch 1966) and with the travel-time data by the relation

$$\tau(p) = T(p)-pX(p). \tag{4}$$

The function $\tau(p)$ is monotonically decreasing, and continuous everywhere except at a finite number of points $p = q_i$ corresponding to the low velocity zones. At these points it has a negative jump σ_i:

$$\sigma_i = \int_{\bar{y}_i}^{\hat{y}_i} [u^2(y)-q_i^2]^{\frac{1}{2}}\,dy. \tag{5}$$

Thus σ_i is characteristic of the magnitude of the low velocity zone.

Let $\omega(p)$ be a piecewise constant function:

$$\omega(p) = \sum_i \sigma_i \quad \text{for} \quad q_i > p. \tag{6}$$

Then

$$\hat{\tau}(p) = \tau(p)-\omega(p) \tag{7}$$

is continuous and

$$\hat{\tau}(p) = \int_p^1 X(q)\,dq \tag{8}$$

(Gerver & Markushevitch 1967). Therefore

$$\tau'(p) = -X(p) \tag{9}$$

if $p \neq q_i$ and $X(p)$ exists.

If we know $\tau(p)$ then except at a finite number of points we know $X(p)$ and $T(p)$:

$$X(p) = -\tau'(p) \quad \text{and} \quad T(p) = \tau(p)+pX$$

(see Gerver & Markushevitch 1966, Section 10).

The function $\tau(p)$ has a simple geometrical interpretation: the tangent of the travel-time curve at the point with co-ordinates $X(p)$, $T(p)$ is characterized by a slope p and time intercept $\tau(p)$.

The function $\tau(p)$ has one important characteristic in the language of differential equations. If we consider the relation (4) as an equation for $\tau(p)$, then using (9) we can write (4) in the form:

$$\tau = p\tau' + T(-\tau'). \tag{10}$$

This is Clairaut's equation (see Appendix); its general solution is a one-parameter family of straight lines:

$$\tau = Cp + T(C). \tag{11}$$

Equation (10) also has one singular solution—it is the envelope of the family of curves (11). Thus we have a definition of the function $\tau(p)$: if we take the Clairaut equation (10) with the travel-time curve as a free term, then the singular solution of this equation is $\tau(p)$. This definition of $\tau(p)$ is important because it does not involve the use of a parametric form of travel-time curve strongly connected with p.

In Section 5 below, this definition of $\tau(p)$ will be used for stable estimation of $\tau(p)$ from a discrete number of points on the travel-time curve. But first, in Sections 3 and 4 we shall show how to obtain the envelope of velocity-depth curves from given estimates of the function $\tau(p)$.

3. Transformation of limits for $\tau(p)$ into limits for $Y(p)$

The Herglotz–Wiechert equation gives the depth corresponding to a given velocity in terms of the function $X(p)$. However, it is $\tau(p)$ and not $X(p)$ that we can estimate from the travel-time curves. Thus it is essential to construct the first term in (2):

$$\phi(p) = 2\pi^{-1} \int_p^1 X(q)[q^2 - p^2]^{-\frac{1}{2}}\, dq. \tag{12}$$

To substitute $\tau(q)$ for $X(q)$ we average $\phi(p)$ in some interval (a, b), $0 < a < b \leqslant 1$:

$$\tilde{\phi}(a, b) = (b-a)^{-1} \int_a^b \phi(p)\, dp = 2\pi^{-1}(b-a)^{-1} \int_a^b \int_p^1 X(q)[q^2 - p^2]^{-\frac{1}{2}}\, dq\, dp \tag{13}$$

$\phi(p)$ is limited in the interval (a, b), so the integral exists. The function $X(q)[q^2 - p^2]^{-\frac{1}{2}}$ is summable, i.e. the integral

$$\int\int_{\mathscr{D}} \frac{X(q)}{(q^2 - p^2)^{\frac{1}{2}}}\, dq\, dp$$

exists for every domain $\mathscr{D}$ in the area $a \leqslant p \leqslant b$, $p \leqslant q \leqslant 1$. In this case we can interchange the order of integration:

$$\tilde{\phi}(a, b) = 2\pi^{-1}(b-a)^{-1} \int_a^1 X(q) \int_a^{\min(q,\, b)} [q^2 - p^2]^{-\frac{1}{2}}\, dq\, dp$$

$$= 2\pi^{-1}(b-a)^{-1} \int_a^1 X(q)\, \alpha(q; a, b)\, dq \tag{14}$$

where

$$\alpha(q; a, b) = \begin{cases} \cos^{-1}(a/q) & \text{if } a \leqslant q \leqslant b \\ \cos^{-1}(a/q) - \cos^{-1}(b/q) & \text{if } b \leqslant q \leqslant 1. \end{cases} \tag{15}$$

The function $\alpha(q)$ increases in the interval (a, b) and decreases in the interval $(b, 1)$.

Now we integrate the expression (14) by parts, using equation (8):

$$\int_a^1 X(q)\,\alpha(q;a,b)\,dq = -\hat{\tau}(q)\,\alpha(q;a,b)\Big|_a^1 + \int_a^1 \hat{\tau}(q)\,\alpha_q'(q;a,b)$$

$$= \int_a^1 \tau(q)\,\beta(q;a,b)\,dq - \sum_{q_i>a} \sigma_i\,\alpha(q_i;a,b) \tag{16}$$

where

$$\beta(q;a,b) = \alpha_q'(q;a,b) = \begin{cases} aq^{-1}[q^2-a^2]^{-\frac{1}{2}} & \text{if } a \leqslant q \leqslant b \\ aq^{-1}[q^2-a^2]^{-\frac{1}{2}} - bq^{-1}[q^2-b^2]^{-\frac{1}{2}} & \text{if } b \leqslant q \leqslant 1. \end{cases} \tag{17}$$

The term outside the integral is zero, because $\hat{\tau}(1) = 0$ and $\alpha(a; a, b) = 0$; the last sum is obtained by direct integration using (6) and (7). Thus we have:

$$\tilde{\phi}(a,b) = \phi_1(a,b) - \phi_2(a,b) \tag{18}$$

where

$$\phi_1(a,b) = 2\pi^{-1}(b-a)^{-1} \int_a^1 \tau(q)\,\beta(q;a,b)\,dq \tag{19}$$

$$\phi_2(a,b) = 2\pi^{-1}(b-a)^{-1} \sum_{q_i>a} \sigma_i\,\alpha(q;a,b) \tag{20}$$

$\alpha(q; a, b)$ and $\beta(q; a, b)$ are defined by (15) and (17). $\phi_2(a, b)$ is related to the low velocity zones; we shall investigate it in the next section. Now we shall estimate $\phi_1(a, b)$.

Suppose that in the interval $(d, 1)$ we know two functions $\dot{\tau}(p)$ and $\bar{\tau}(p)$ such that:

$$\bar{\tau}(p) \leqslant \tau(p) \leqslant \dot{\tau}(p) \quad \text{for} \quad 0 < d \leqslant p \leqslant 1. \tag{21}$$

We have from (17):

$$\left.\begin{aligned} \beta(q;a,b) > 0 \qquad & \text{for } a < q < b \\ \beta(q;a,b) < 0 \qquad & \text{for } b < q < 1. \end{aligned}\right\} \tag{22}$$

It follows from (19), (21) and (22) that if $d \leqslant a$, then

$$2\pi^{-1}(b-a)^{-1} \int_a^1 \bar{\eta}(q;a,b)\,\beta(q;a,b)\,dq \leqslant \phi_1(a,b)$$

$$\leqslant 2\pi^{-1}(b-a)^{-1} \int_a^1 \dot{\eta}(q;a,b)\,\beta(q;a,b)\,dq \tag{23}$$

where

$$\dot{\eta}(q;a,b) = \begin{cases} \dot{\tau}(q) & \text{for } a < q < b \\ \bar{\tau}(q) & \text{for } b < q < 1 \end{cases} \tag{24a}$$

$$\bar{\eta}(q;a,b) = \begin{cases} \dot{\tau}(q) & \text{for } a < q < b \\ \bar{\tau}(q) & \text{for } b < q < 1. \end{cases} \tag{24b}$$

If $\dot{\tau}(p)$ and $\bar{\tau}(p)$ were piecewise linear functions, the integrals in (23) could be calculated in explicit form.

Now we have to pass from the estimates (23) over average values to the estimates of $Y(p)$. Since $Y(p)$ is monotonically decreasing, we have:

$$Y(b) < \tilde{Y}(a,b) < Y(a) \tag{25}$$

where

$$\tilde{Y}(a,b) = (b-a)^{-1} \int_a^b Y(p)\,dp.$$

$\tilde{Y}(a,b)$ can be represented as the difference between $\phi_1(a,b)$ and the term connected with low velocity zones (equations (32) and (33)). In this section we consider velocity-depth curves without low velocity zones, so that $\tilde{Y}(a,b) = \phi_1(a,b)$; in Section 4 we shall correct the estimates of $\tilde{Y}(a,b)$ to allow for low velocity zones.

Let us take the upper estimate

$$Y(b) < \tilde{Y}(a,b) < 2\pi^{-1}(b-a)^{-1} \int_a^1 \dot{\eta}(q;a,b)\,\beta(q;a,b)\,dq. \tag{26}$$

We fix the inverse velocity b, and our problem is to find an optimal averaging interval (a,b) so that the estimate (26) would be best in some sense. For a very small interval (a,b) the second inequality in (26) gives a very crude estimate, because the right-hand term in (26) tends to infinity if $a \to b$. Increasing the interval (a,b), the estimate (26) is at first improved because the difference between the integral and $\tilde{Y}(a,b)$ decreases; further on it deteriorates because the difference $\tilde{Y}(a,b) - Y(b)$ increases; thus it is not difficult for us to find an optimal averaging interval.

We start with an averaging interval of 0·01. If 0·02 gives a better estimate (26) than 0·01, then we try 0·03, 0·04, etc., until the estimate (26) is improved; otherwise we try 0·005, 0·0025, etc. In an analogous way we can find an optimal averaging interval (a,b) for the lower estimate given by the equation

$$Y(a) > \tilde{Y}(a,b) > 2\pi^{-1}(b-a)^{-1} \int_a^1 \bar{\eta}(q;a,b)\,\beta(q;a,b)\,dq. \tag{27}$$

So we have the following algorithm: we step along the p-axis from 1 to d, where d is specified by (21). For each value of p we look for optimal averaging intervals for lower and upper estimates, and then we calculate estimates of $Y(p)$ by equations (26) and (27).

4. Low velocity zones

Let us now take the second term in equation (2):

$$\Psi(p) = \sum_{q_i > p} 2A_i(p)/\pi \tag{28}$$

where

$$A_i(p) = \int_{\bar{y}_i}^{\dot{y}_i} \tan^{-1}\{[u^2(y) - q_i^2]/[q_i^2 - p^2]\}^{\frac{1}{2}}\,dy. \tag{29}$$

We shall use the averaged function:

$$\tilde{\Psi}(a,b) = \sum_{q_i > a} 2\tilde{A}_i(a,b)/\pi \tag{30}$$

where

$$A_i(a,b) = (b-a)\int_a^b A_i(p)\,dp. \tag{31}$$

It follows from (2) and (18) that

$$\tilde{Y}(a,b) = \tilde{\phi}(a,b)+\tilde{\Psi}(a,b) = \phi_1(a,b)-\Psi_1(a,b) \tag{32}$$

where

$$\Psi_1(a,b) = \phi_2(a,b)-\tilde{\Psi}(a,b). \tag{33}$$

Now we have to estimate $\Psi_1(a, b)$. It is sufficient to investigate the single summand $B_i(a, b)$ corresponding to the ith low velocity zone:

$$\Psi_1(a,b) = 2\pi^{-1}\sum_{q_i>a} B_i(a,b) \tag{34}$$

$$B_i(a,b) = (b-a)^{-1}\,\sigma_i\,\alpha(q_i;a,b)-\tilde{A}_i(a,b). \tag{35}$$

We assume that the interval (a, b) does not contain a low velocity zone, i.e. $q_i > b$. Then

$$\alpha(q_i;a,b) = \cos^{-1}(a/q_i)-\cos^{-1}(b/q_i). \tag{36}$$

Let $\Pi_i(p)$ denote a functional of $A_i(p)$, $\Pi_i'(p) = A_i(p)$. Then

$$A_i(a,b) = (b-a)^{-1}\,[\Pi_i(b)-\Pi_i(a)]. \tag{37}$$

It follows from (35), (36) and (37) that

$$B_i(a,b) = (b-a)^{-1}\{[\sigma_i\cos^{-1}(a/q_i)+\Pi_i(a)]-[\sigma_i\cos^{-1}(b/q_i)+\Pi_i(b)]\}. \tag{38}$$

According to Lagrange's theorem there exists a number ξ, $a < \xi < b$, such that

$$B_i(a,b) = \sigma_i(q_i^2-\xi^2)^{-\frac{1}{2}}-A_i(\xi). \tag{39}$$

Considering (5) and (29), we have:

$$B_i(a,b) = \int_{\bar{y}_i}^{\dot{y}_i} [Q_i-\tan^{-1}Q_i]\,dy \tag{40}$$

where

$$Q_i = \{[u^2(y)-q_i^2]/[q_i^2-\xi^2]\}^{\frac{1}{2}}. \tag{41}$$

One of the advantages of our method compared to using equation (2) is that $B_i(a, b) \ll \tilde{A}_i(a, b)$, i.e. as the depth below the low velocity zone increases, $B_i(a, b)$ decreases proportionally to Q_i^3, whereas $A_i(p)$ decreases only as Q_i.

Since $Q_i > \tan^{-1} Q_i$, we have $B_i(a, b) > 0$ and $\Psi(a, b) > 0$. Hence the upper estimate (26) could only improve in the presence of a low velocity zone.

In (39) the minuend is independent of the velocity distribution within the low velocity zone for fixed σ_i. As to the subtrahend, the following statement can be formulated (it follows from the convexity of the function $\tan^{-1} X$; for details see Markushevitch & Reznikov 1973). This subtrahend is minimal for the deepest possible, and correspondingly most narrow, rectangular low velocity zone, i.e. for the case when the velocity is constant and as small as possible. It is maximal for the widest shallow rectangular low velocity zone.

For a rectangular low velocity zone, equation (40) can be written

$$\dot{B}_i(a,b) = \sigma_i(b-a)^{-1}\,[1-Q_i^{-1}\tan^{-1}Q_i]. \tag{42}$$

Now we need estimates of the parameters σ_i, q_i, Q_i.

As will be shown in Section 5, we can find values $\dot{q}_i$, $\bar{q}_i$, $\dot{\sigma}_i$, and $\bar{\sigma}_i$ such that

$$\bar{q}_i \leqslant q_i \leqslant \dot{q}_i \qquad \bar{\sigma}_i \leqslant \sigma_i \leqslant \dot{\sigma}_i \tag{43}$$

from the estimates of $\tau(p)$ given by $\dot{\tau}(p)$ and $\bar{\tau}(p)$.

Now we assume that the velocity in the ith low velocity zone is greater than some given value V_i:

$$V_i < V(y) \quad \text{for} \quad \bar{y}_i < y < \dot{y}_i.$$

We write $\dot{u}_i = 1/V_i$. Since the function $Q_i^{-1} \tan^{-1} Q_i$ decreases monotonically, we have the following upper estimate of $B_i(a, b)$:

$$B_i(a,b) \leqslant \dot{\sigma}_i[\bar{q}_i^2 - \xi^2]^{-\frac{1}{2}} [1 - \dot{Q}_i^{-1} \tan^{-1} \dot{Q}_i] \tag{44}$$

where

$$\dot{Q}_i = \{[\dot{u}_i^2 - \bar{q}_i^2]/[\bar{q}_i^2 - \xi^2]\}^{\frac{1}{2}}. \tag{45}$$

We can get a final lower estimate for $Y(p)$ from (27), (32), (34) and (44).

The lower estimate for $B_i(a, b)$ corresponds to the widest and shallowest rectangular low velocity zone for a given σ_i. The upper estimate $\dot{h}_i$ for the width of the ith low velocity zone can be obtained as follows: $\dot{h}_1$ is equal to the supremum of the difference between the upper and lower estimates of $Y(p)$ in the interval $(\bar{q}_1, \dot{q}_1)$, given by (26) and (27). Further on we can use induction. Suppose we have upper and lower estimates for $Y(p)$ with allowance for the first $i-1$ low velocity zones. Then $\dot{h}_i$ is equal to the supremum of the difference between these estimates in the interval $(\bar{q}_i, \dot{q}_i)$. Determining h_i in this way we can calculate the lower estimate $\bar{u}_i$ for $u(y)$ in the interval $(\bar{y}_i, \dot{y}_i)$ from the relation

$$\bar{\sigma}_i = \dot{h}_i[\bar{u}_i^2 - \dot{q}_i^2]^{\frac{1}{2}}.$$

Now we have the lower estimate for $B_i(a, b)$:

$$B_i(a,b) \geqslant \bar{\sigma}_i[\dot{q}_i^2 - \xi^2]^{-\frac{1}{2}} [1 - \bar{Q}_i^{-1} \tan^{-1} \bar{Q}_i] \tag{46}$$

where

$$\bar{Q}_i = \{[\bar{u}_i^2 - \dot{q}_i^2]/[\dot{q}_i^2 - \xi^2]\}^{\frac{1}{2}}. \tag{47}$$

Hence we get the final upper estimate for $Y(p)$ from (26), (32), (34) and (46).

If the interval (a, b) contains a low velocity zone, i.e. $q_i < b$, we take the lower estimate that is constant and equal to the existing estimate at the point b; the upper estimate remains unaffected.

We use the average values $B_i(a, b)$ for estimates of $Y(p)$ at the ends of the interval (a, b); consequently we can take for our calculations $\xi = \frac{1}{2}(a+b)$ in (44)–(47).

From estimates of $Y(p)$ obtained in this way, we can calculate estimates of the function $V(y)$ outside the low-velocity zones. In addition, we know the domains in the (V, y) plane containing low velocity zones, and the estimates of σ_i which are characteristic of the magnitude of the low velocity zones. However, we do not know anything about the velocity distribution within the low velocity zones.

It remains to carry out the most interesting and most difficult part, namely to get estimates of $\tau(p)$ from given travel-time data.

5. Transformation of $T_i(X_i)$ into limits for $\tau(p)$

Suppose we have a discrete number of exact travel-time data, namely the epicentral distances X_i and the corresponding travel times $T_i = T(X_i)$. We want to transfer this information to the (τ, p) plane. Each point (T_i, X_i) of a travel-time curve corresponds to the straight line l_i with slope $-X_i$ and time intercept T_i in the (τ, p) plane. Each l_i is the tangent of the graph $\tau(p)$. Thus our problem is to construct the envelope of the set of straight lines l_i; each of these lines is given by the equation

$$\tau = T_i - pX_i. \tag{48}$$

This problem can be reformulated using the Clairaut equation. We have the set of particular solutions (48) of the equation

$$\tau(p) = p\tau'(p) + T(-\tau') \tag{49}$$

and the problem is to find its singular solution.

Unfortunately an arbitrary curve cannot be properly determined by a finite number of its tangents, and there is no stable dependence in the metric of the space C between the arbitrary free term of the Clairaut equation—$T(X)$ in our case—and its singular solution. Our purpose is to find a stable dependence between $T(X)$ and $\tau(p)$ by use of the characteristic properties of the travel-time curve and of the function $\tau(p)$.

We need the following definition: suppose that the observed $T(X_i)$ in some interval of X can be connected by a curve which is convex upwards or downwards. We shall call the travel-time curve on such an interval a generally direct or generally receding branch respectively.

Let us now give the definition of a loop. We consider a single-valued function $T_*(X) = \inf_X T(X)$ for a generally direct branch of the travel-time curve and $T^*(X) = \sup_X T(X)$ for a generally receding branch. Then a loop is some connected subset of the graph $T(X)$ which does not belong to the graph $T^*(X)$ or $T_*(X)$. We do not know anything about small loops from our discrete travel-time data, but the following consideration shows how to construct an envelope in the (τ, p) plane which contains the graph $\tau(p)$, whether or not there are loops in the travel-time curve.

We suppose that we know some general branch of the travel-time curve in the metric of the space C., i.e. there is a sufficiently narrow band L in the (T, X) plane which contains our general branch with given $T_i(X_i)$: see Fig. 1. We assume that the

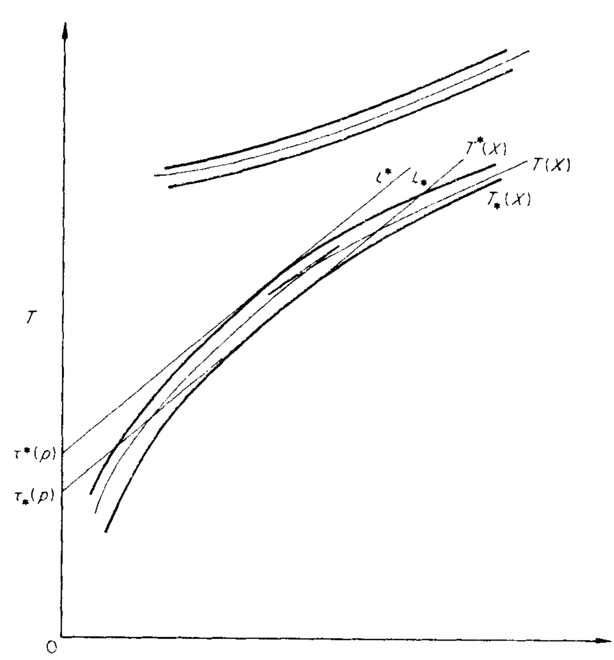

FIG. 1. Construction of $\tau(p)$ from $T(X)$.

band L is limited by two monotone smooth convex functions $\bar{T}(X)$ and $\dot{T}(X)$, i.e. all necessary conditions are satisfied for $\bar{T}(X)$ and $\dot{T}(X)$ to be a continuous branch of the travel-time curve without loops. Let $D(X) = \dot{T}(X) - \bar{T}(X)$.

We shall consider below the case of the generally direct branches of the travel-time curve, so that $\dot{T}(X)$ and $\bar{T}(X)$ are convex upwards; the case of generally receding branches can be considered in an analogous way.

We shall now describe how to estimate the limits of $\tau(p)$ from the band L.

Let l be a tangent (with slope p) of the travel-time curve at some point which lies within the band L. It is clear that l lies between two parallel tangents: $\bar{l}$ of $\bar{T}(X)$ and $\dot{l}$ of $\dot{T}(X)$. The time intercept of l is $\tau(p)$; therefore $\tau(p)$ is limited by two time intercepts: $\bar{\tau}(p)$ of $\bar{l}$ and $\dot{\tau}(p)$ of $\dot{l}$. We have:

$$\delta(p) = \dot{\tau}(p) - \bar{\tau}(p) \leqslant \max\,[D(X^*), D(X_*)]$$

where X^* and X_* are abscissas of the points of tangency $\dot{l}$ with $\dot{T}$ and $\bar{l}$ with $\bar{T}(X)$, respectively. It gives us a stable dependence of $\tau(p)$ on $T(X)$ in the metric of the space C.

This theoretical result emphasizes the basic role of the function $\tau(p)$. The construction of the band L from real data presents many difficulties, but it is not necessary for estimation of $\tau(p)$. Let us fix p_0 and consider the function $\tau(X, p_0)$:

$$\tau(X, p_0) = T(X) - p_0 X.$$

This function is similar to the reduced travel time often used in seismology. We have:

$$\tau_X'(X, p_0) = p(X) - p_0$$

$p(X)$ is a multivalued function. There is a unique point $T_0 = T(X_0)$ of the travel-time curve for which $p(X_0) = p_0$. Therefore $\tau_X'(X, p_0)$ has a single zero and $\tau(X, p_0)$ has a single stationary point, which is a maximum for the generally direct and a minimum for the generally receding branch of the travel-time curve. We have:

$$\tau(X_0, p_0) = T_0 - p_0 X_0 = \tau(p_0),$$

i.e. the extreme value of $\tau(X, p_0)$ is $\tau(p_0)$.

Thus we use the following algorithm: we select a general branch of the travel-time curve—let $T_i, X_i, i = 1, 2, \ldots, n$ be the given data on this branch. Then we find

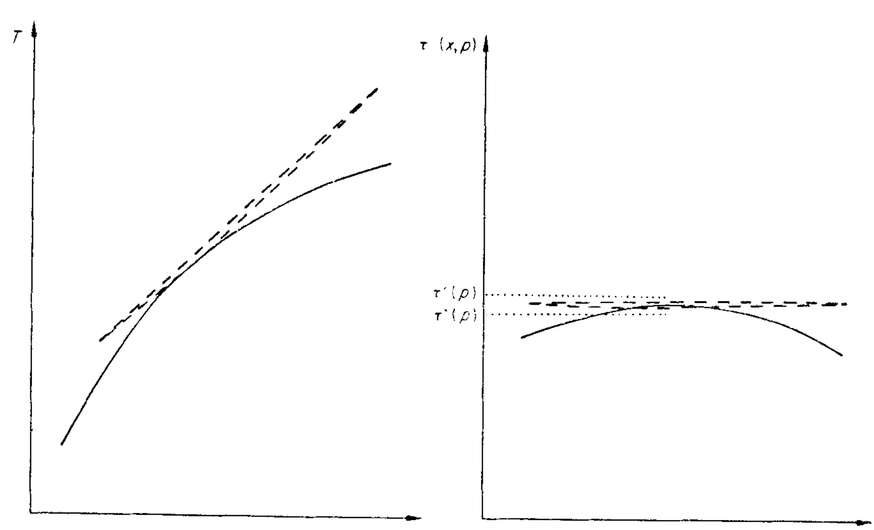

FIG. 2. Large loop on the travel-time curve.

an interval of p where $\tau(X, p)$ has an extremum, and for values p_k in this interval, with some finite step size we construct the set of points $\tau(X_i, p_k) = T_i - p_k X_i$, $i = 1, 2, \ldots, n$. From this set we estimate the extreme values of the function $\tau(X, p_k)$, and this is our estimate for $\tau(p_k)$. Due to the monotone character of $\tau(p)$ we are able to construct the band M in the (τ, p) plane which contains the curve $\tau(p)$. The error in $\tau(p_k)$ does not exceed the error in T_i plus p_k times the error in X_i; i.e. the error in $\tau(p)$ is of the same order as the error in $T(X)$. Notice that even the presence of large unnoticed loops in the travel-time curve does not damage the estimates of $\tau(p)$ obtained in this way (see Fig. 2). If $\tau(X, p_k)$ reaches an extremum for $X = X_k$, we have $X(p_k) \approx X_k$, but the error in this condition can be rather large. It is noteworthy that the method of estimation of $\tau(p)$ described above is simply a convenient procedure for solving the Clairaut equation (49).

The estimates of the function $\tau(p)$ between two neighbouring bands M_1 and M_2 corresponding to two consecutive branches of the travel-time curve can be calculated by the 'method of parallelgrams' using the estimates of $X(p)$ in this interval (Bessonova *et al.* 1970; Keilis-Borok 1971). Three cases are shown in Fig. 3; they differ in the existence of non-existence of gaps in τ and p between M_1 and M_2:

(1) There are no gaps in p and τ. This means that we have no evidence of a low velocity zone.

(2) There are some gaps in p and τ. We cannot prove that a low velocity zone exists, but we have to take into account that this zone may exist in the interval $(\bar{q}, \dot{q})$ with $\sigma \leqslant \dot{\sigma}$.

(3) There is no gap in p, but there is a gap in τ. If we have estimates of $X(p)$, we can prove that a low velocity zone exists in the interval $(\bar{q}, \dot{q})$, with $\bar{\sigma} < \sigma < \dot{\sigma}$.

In cases (2) and (3) we use the values $\bar{q}$, $\dot{q}$, $\bar{\sigma}$, $\dot{\sigma}$ for estimates of the summand connected with the low velocity zones in the expression for $Y(p)$ (see Section 4).

In this way we get the envelope in the (τ, p) plane which contains the graph of the function $\tau(p)$; its upper boundary is the graph of $\dot{\tau}(p)$ and its lower boundary is the graph of $\bar{\tau}(p)$. As we have seen in Sections 3 and 4, this information is sufficient for construction of the envelope in the (V, Y) plane which contains all velocity-depth curves consistent with the given travel-time data.

In Sections 6–8 we shall apply this 'τ method' to deep seismic sounding for investigating the velocity distribution in the Earth's crust.

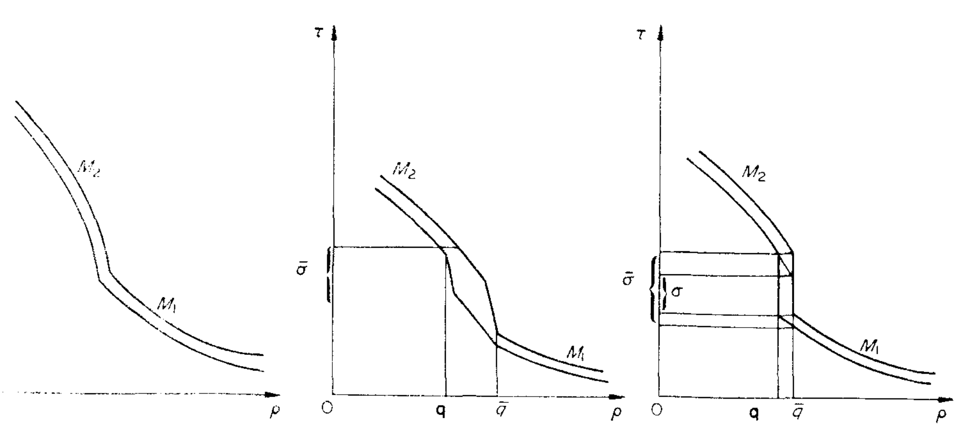

FIG. 3. Estimation of the existence of wave guides from $\tau(p)$.

6. Experimental data

In 1962–1964 detailed deep seismic sounding along profiles was carried out in Central Turkmenia (Ryaboyi 1966a, b). Body waves recorded at distances up to 300 km have propagated through media which for all practical purposes are horizontally homogeneous (after introducing near-surface time corrections). The recordings were made along a set of parallel and reversed profiles; the average difference between times on reversed profiles is about 0·1 s. The horizontal homogeneity allows us to apply the 'τ method'.

Let us describe the observed waves. The first arrivals at distances up to about 10–12 km correspond to the sedimentary layers. Between 10–12 km and 120–125 km the first arrivals correspond to refracted p_0 waves, which propagate in the upper part of the consolidated crust (Fig. 4).

P_0 waves are characterized by intensive and prolonged oscillations; their phase correlation is continuous for distances of several dozen kilometres.

In the later arrivals two basic groups of waves appear. These are the waves reflected from the bottom of the crust (P_1^M) and from a boundary in the lower part of the consolidated crust (P_2). The P_1^M and P_2 waves have intensive arrivals. They are well correlated along the profile and can easily be identified on the parallel and reversed profiles. The P_2 and P_1^M waves can be followed from 50 to 60 km up to 150–170 km and 280–290 km, respectively.

Between P_0 and P_2 a considerable number of weak unclear arrivals exist, with a short range of correlation. We shall designate these waves as P_1. The apparent velocities of these waves are intermediate between those of P_0 and P_2 waves. The

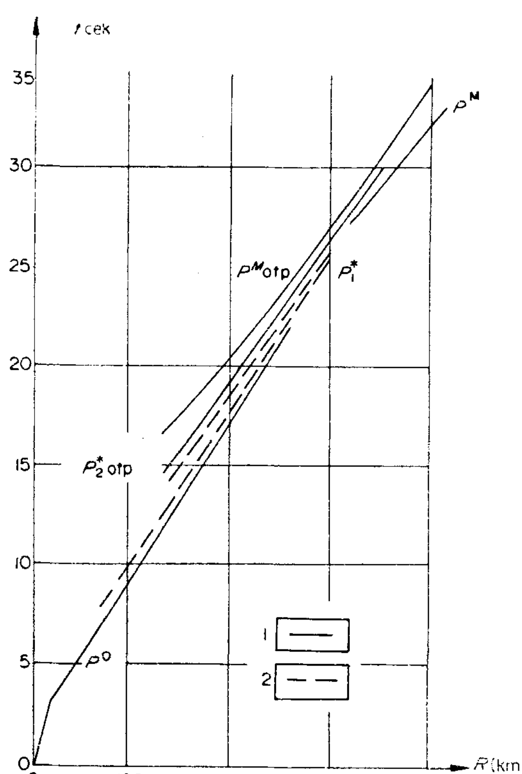

FIG. 4. Scheme of travel-time curves of main recorded waves: (1) Basic waves, reliably separated and correlated; (2) p_1 waves, with small amplitude and poor correlation.

physical nature of the P_1 waves is unclear. Possibility they are reflections from heterogeneities in the middle part of the consolidated crust. After the disappearance of P_0 waves at 120–125 km, the P_1 waves appear as first arrivals up to 150–160 km. Further on, waves refracted in the upper mantle (P_2^M) appear as first arrivals.

7. Application of the ' τ Method '

As initial data we use the travel times of first arrivals and the travel times of P_2 and P_1^M waves for epicentral distances at intervals of 5 km. The accuracy of the travel times is less than 0·1 s. The velocity at the free surface, $V(0)$, is assumed to be 1·25 km s^{-1}; therefore $p = 1{\cdot}25/V(y)$. We have to obtain an estimate of the function $\bar{\tau}(p)$ by the methods described in Section 5. First of all we shall investigate the travel-time curve of the first arrivals at distances from 10 to 205 km. To eliminate the influence of local near-surface inhomogeneities we smoothed the travel time, replacing each arrival time by the average of five successive points. For the smoothed data we plot $\tau_i = T_i - pX_i$ *vs.* X for $0{\cdot}23 \leqslant p \leqslant 0{\cdot}145$, at an interval of 0·0025 (Fig. 5). Since T_i and X_i are one-half the time and distance values, the error in T_i is less than 0·05. As these curves possess more than one extremum it follows that in the first arrivals several different waves are present. Let us try to separate them.

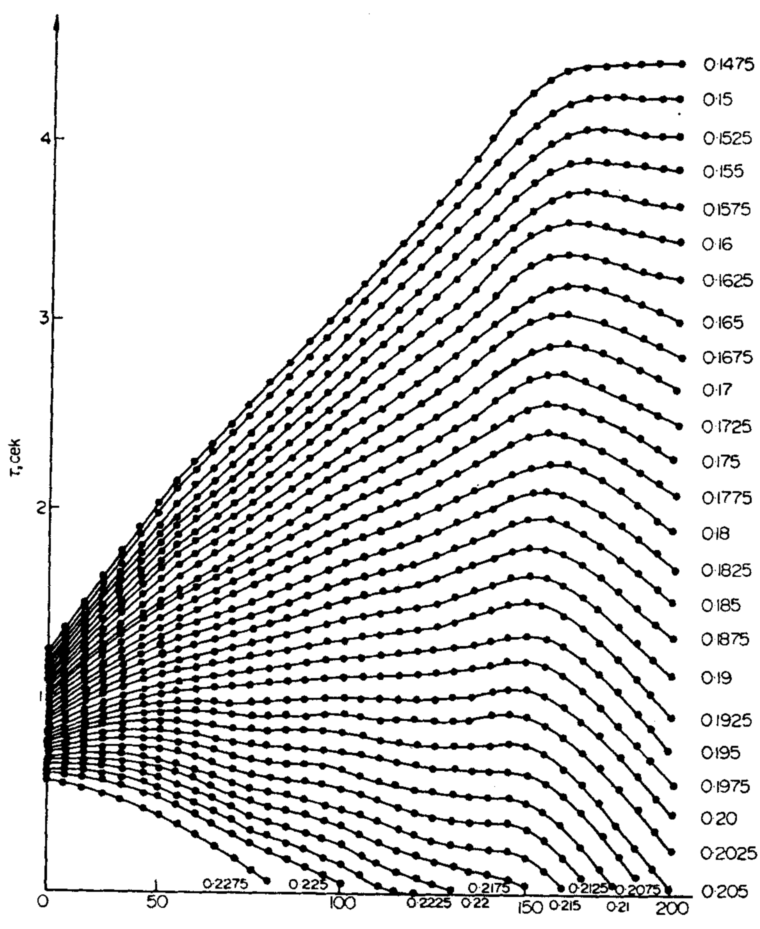

FIG. 5. $\tau(X, p)$ for different p, corresponding to first arrivals.

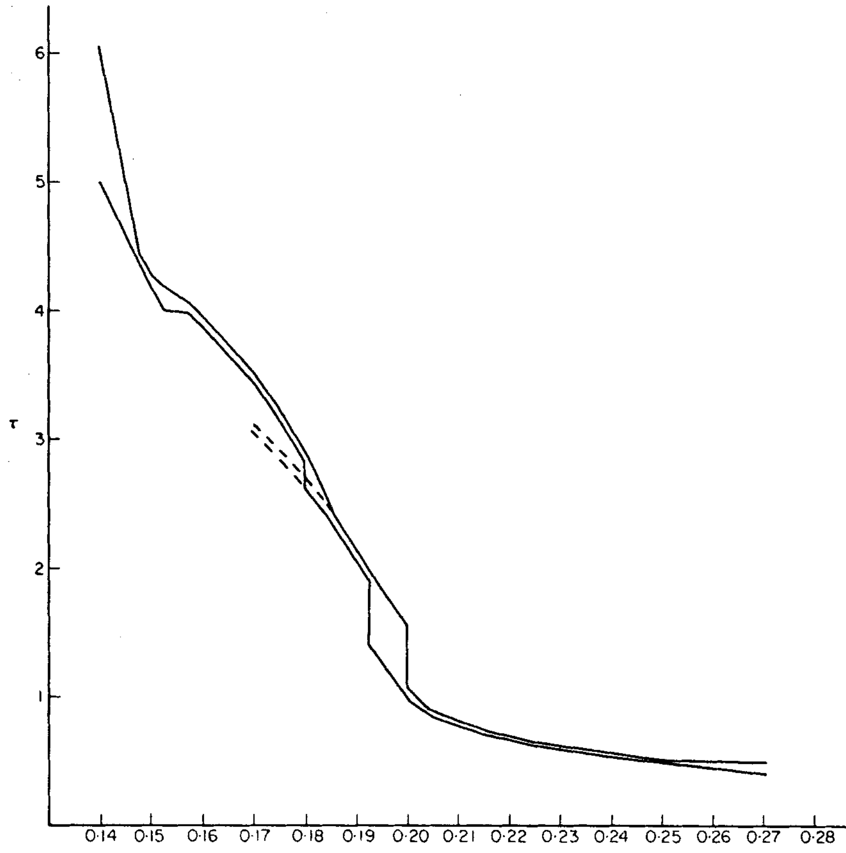

FIG. 6. Estimation of $\tau(p)$ in the p interval corresponding to waves propagating through the Earth's crust.

From Fig. 5 it is not difficult to see that the behaviour of $\tau(X, p)$ is regular at distances from 10 to 110 km ($0{\cdot}20 \leqslant p \leqslant 0{\cdot}23$). Apparently here we have P_0 waves (see Section 6). Their apparent velocity changes from 5·6 to 6·3 km s^{-1}. In accordance with the theory described in Section 5, the maxima of the derived curves shifts along the diagonal from the lower left corner to the upper right corner. The value of the maximum is determined with error less than 0·05. Then on the (τ, p) plane we construct a band of average width 0·06 containing the graph $\tau(p)$ in the interval $0{\cdot}2 \leqslant p \leqslant 0{\cdot}225$.

The estimates of $\tau(p)$ for $0{\cdot}20 \leqslant p \leqslant 0{\cdot}225$ obtained in this way are shown in Fig. 6.

Further we are able to single out the regular behaviour of $\tau(X, p)$ at distances from 160 to 200 km ($0{\cdot}145 \leqslant p \leqslant 0{\cdot}155$); see Fig. 6. These are $P_2{}^M$ waves; their apparent velocity changes from 8·1 to 8·4 km s^{-1}. The estimates of the $\tau(p)$ for p values close to 0·15 are obtained in an analogous way. They are shown in Fig. 6.

The curves $\tau(X, p)$ for X between 120 and 150 km are irregular and cannot be interpreted in this way. One must remember that at these distances, P_1 waves appear as first arrivals; their nature was discussed in Section 6. We exclude these waves from the travel-time curve and do not consider them further.

It is useful to compare the results obtained in this way with the results obtained by the usual method of interpreting deep seismic sounding data. For that we shall choose the times of the first arrivals from 10 to 205 km with an even smaller interval:

one kilometre. We shall try to obtain values of the ray parameter p by differentiating the travel-time curve. We know the exact values of X_i, so assuming that the errors in calculating T_i are independent and normally distributed we can determine p_i by the technique of statistical regression. Through each five successive points (T_i, X_i) we draw a polynomial of the third or smaller order using least squares; the value of the polynomial at the middle point we assume as T_i; differentiating the polynomial with respect to X we obtain the values of p_i at the middle point. Determining p_i at each point in this way we make the errors in p_i not independent, but still normally distributed. The cloud of points obtained for $p_i(X_i)$ is shown in Fig. 7; in Fig. 8, the corresponding cloud of points $\tau_i(p_i) = T_i - p_i X_i$ is shown.

We see that the condition of monotonicity of the function $\tau(p)$ is rudely violated, so it is evident that the values of $\tau_i(p_i)$ are calculated with large errors. The errors in the values of T_i are not large and the error in $\tau_i(p_i)$ is due to the errors in differentiation. Let us in fact take the values of p_i from the function of $X(p)$ obtained not by differentiation, but by our method (see the continuous line in Fig. 7). The values $\tau_i(p_i)$ corresponding to these p_i have small scatter and lie well within a narrow zone, shown in Fig. 7.

Due to the errors in p_i, each point τ_i has moved from its true position along the tangent $\tau = T_i - pX_i$ to the graph of the function $\tau(p)$. The travel-time curve of the first arrivals is generally direct (see Section 5), which is why the graph of the $\tau(p)$ function is convex downwards. In this case all the tangents lie below the graph of $\tau(p)$. Therefore all the τ_i, which are calculated with significantly wrong p_i, also lie below the graph of $\tau(p)$. This explains why the cloud of points in Fig. 8 has a clear upper boundary and a very indefinite lower boundary; it also explains the presence of negative τ_i.

In an analogous way we determined the curves $\tau(X, p)$ for different p corresponding to the P_2 arrivals at distances from 60 to 160 km, with a 5-km interval. The behaviour of these curves is regular for $0{\cdot}075 \leqslant p \leqslant 0{\cdot}195$; it is possible to estimate reliably the minimum points, which we use to calculate $\tau(p)$. The estimates of $\tau(p)$ thus obtained are shown in Fig. 6. The apparent velocity changes from 6·5 to 7·2 km s^{-1}. Later, more comments will be made about why the graph of $\tau(p)$ is shown by a dotted line in the interval $0{\cdot}175 \leqslant p \leqslant 0{\cdot}185$.

We constructed two separate bands of $\tau(p)$; now we have to join them. The joint is of type II (see Section 5), i.e. there is a gap in p from 0·1925 to 0·20, corresponding to the velocity interval 6·3–6·4 km s^{-1}, and a gap in τ from 1·1 to 1·7. The corresponding part of the travel-time curve is not observed, apparently because it corresponds to arrivals with small amplitudes. We can put the graph of the function $\tau(p)$

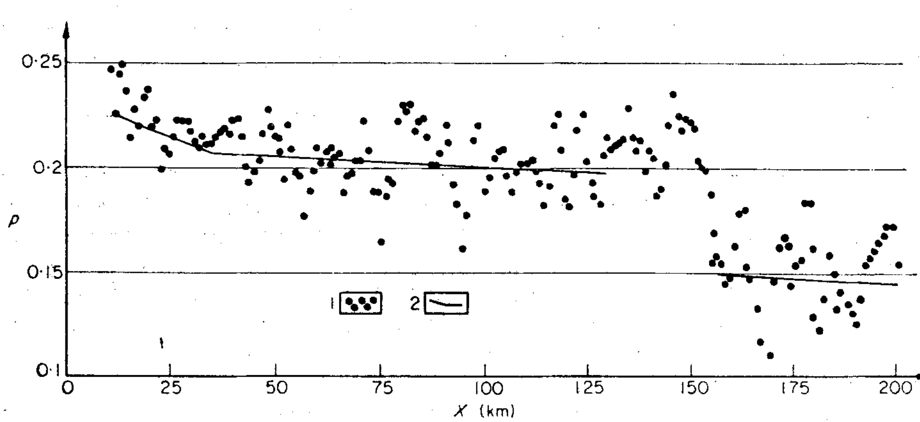

FIG. 7. Derivation of epicentral distance X from the ray parameter p: (1) $X_i(p_i)$ values obtained by numerical differentiation; (2) $X(p)$ obtained by the τ method.

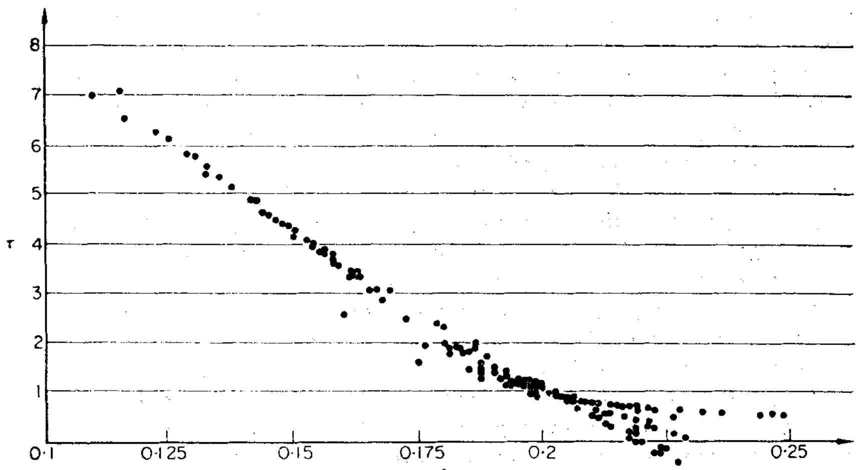

FIG. 8. $\tau_i(p_i)$ values obtained by numerical differentiation.

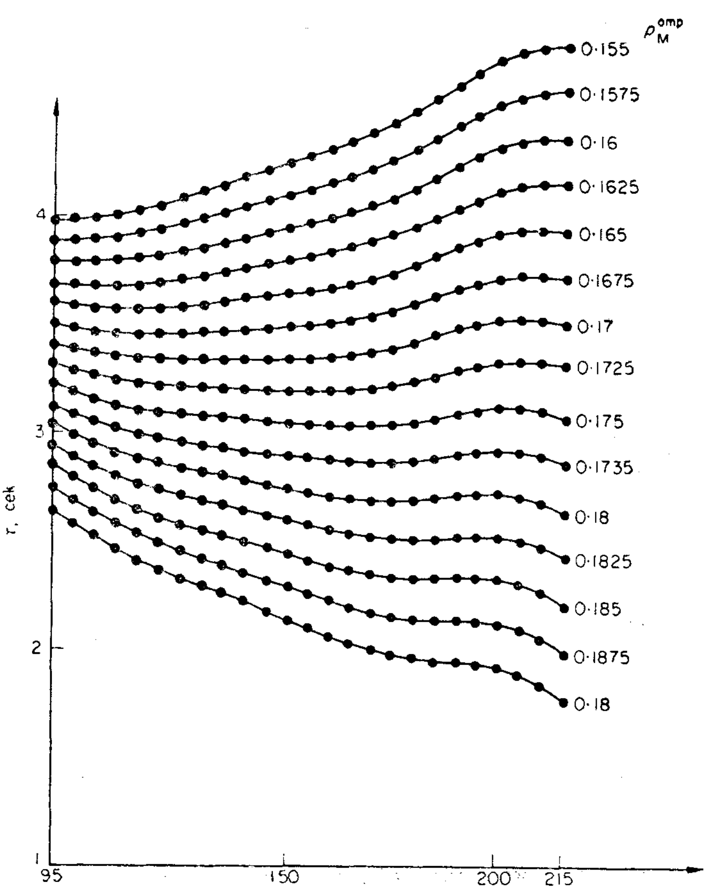

FIG. 9. $\tau(X, p)$ for different p, corresponding to $P_1{}^M$ waves.

inside a parallelogram as shown in Fig. 6; it is constructed according to the assumption that the corresponding part of the travel-time curves goes between 100 and 500 km. We cannot prove that there is a low velocity zone in the examined part of the travel-time curve, but we must take into account the possibility of existence of a low velocity zone in the interval $0{\cdot}1925 \leqslant p \leqslant 0{\cdot}20$. For this low velocity zone, $\sigma < 0{\cdot}5$.

The estimates of $\tau(p)$ calculated in an analogous way from the $P_1{}^M$ wave travel times between 60 and 240 km distance are shown in Fig. 7 for $0{\cdot}155 \leqslant p \leqslant 0{\cdot}185$. The graphs $\tau(X, p)$ for different values of p corresponding to $P_1{}^M$. The apparent velocity changes from $6{\cdot}8\,\mathrm{km\,s^{-1}}$ to $8{\cdot}1\,\mathrm{km\,s^{-1}}$. The way in which this zone joins the two zones already considered is of type I and causes no difficulties.

The splitting of the graph of $\tau(p)$ in the interval 0·175–0·185 (the dotted line in Fig. 6) is explained in the following way. In the lower part of the consolidated crust there is a discontinuity, with a jump in velocity from $6{\cdot}4$–$6{\cdot}5\,\mathrm{km\,s^{-1}}$ to $6{\cdot}75$–$6{\cdot}85\,\mathrm{km\,s^{-1}}$; the rays refracted from this discontinuity form the P_2 branch. The rays corresponding to velocities larger than $6{\cdot}85\,\mathrm{km\,s^{-1}}$ are split at this boundary. According to our theory, in such a case we have to include in the travel-time curve only the refracted wave arrivals and not the reflelcted ones (Gerver & Markushevitch 1966). Therefore we have to use the $P_1{}^M$ branch to estimate $\tau(p)$ in the interval $0{\cdot}175 \leqslant p \leqslant 0{\cdot}185$.

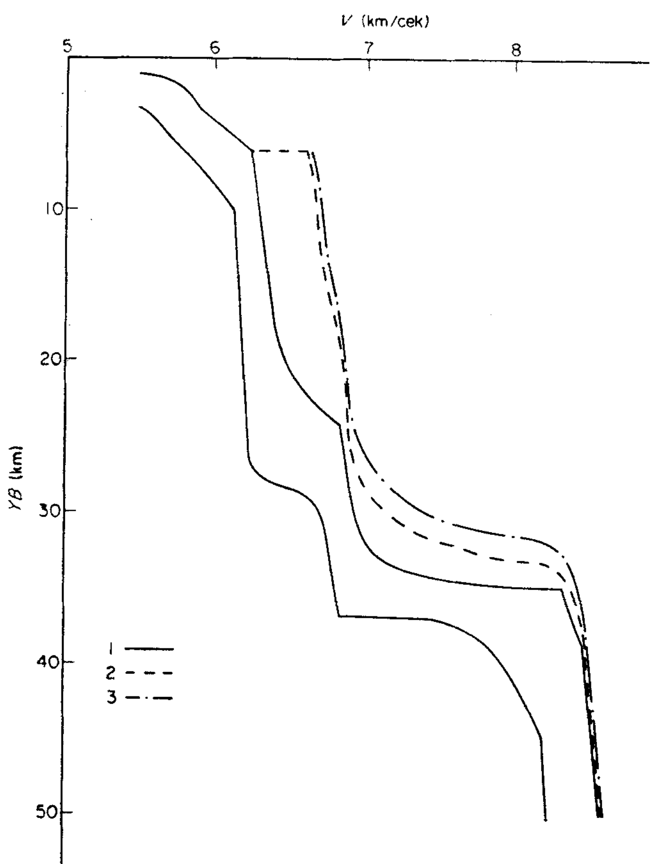

FIG. 10. The area which contains all possible velocity-depth curves: (1) in the absence of wave guides; (2) and (3) lower boundary in the presence of wave guides. The lower limit for velocity inside wave guides is 6 km s^{-1} for (2) and 5·5 km s^{-1} for (3).

Thus we estimated $\tau(p)$ for $0{\cdot}1475 \leqslant p \leqslant 0{\cdot}225$. In order to get information about the velocity-depth curve we must specify the behaviour of the function $\tau(p)$ for $0{\cdot}225 \leqslant p \leqslant 1$. We use borehole data on velocities in the upper two kilometres of the sediments; from these velocities we calculated $\tau(p)$ for $0{\cdot}225 \leqslant p \leqslant 1$. Thus since we have estimates of the function $\tau(p)$ for $0{\cdot}1475 \leqslant p \leqslant 1$ and also some information about low velocity zones, we are able to use the equations of Sections 3 and 4 to build a region containing all the velocity-depth curves corresponding to the examined travel-time data. The result is shown in Fig. 10, which shows the boundaries of the above-mentioned region in the absence of low velocity zones and also in the presence of these zones, for different limits on the velocity in them.

8. Discussion of results

The obtained results (Figs 10 and 11) show the main features of the velocity-depth distribution within the crust, and allow us to determine rather accurately some of its parameters (for example, the thickness of the crust); simultaneously they show that our data do not allow us to determine all the important features of the velocity distribution uniquely. In particular, the question whether low velocity zones exist remains open. This is clearly seen in Fig. 11, which shows three different velocity-depth curves for which the calculated travel times fit the observations, for P_0, P_2, $P_1{}^M$, and $P_2{}^M$ waves with error not exceeding 0·1 s. All the parts of the calculated travel-time curves which are absent on the real observed ones correspond to waves with very small amplitudes. All calculated graphs of $\tau(p)$ are inside the zone we determined (Fig. 6). Note the existence of velocity-depth curves which correspond simultaneously to two kinds of data: (i) observed travel times, and (ii) the function $\tau(p)$, fitting the limits determined by our method. This confirms our calculations of $\tau(p)$ from $T(X)$.

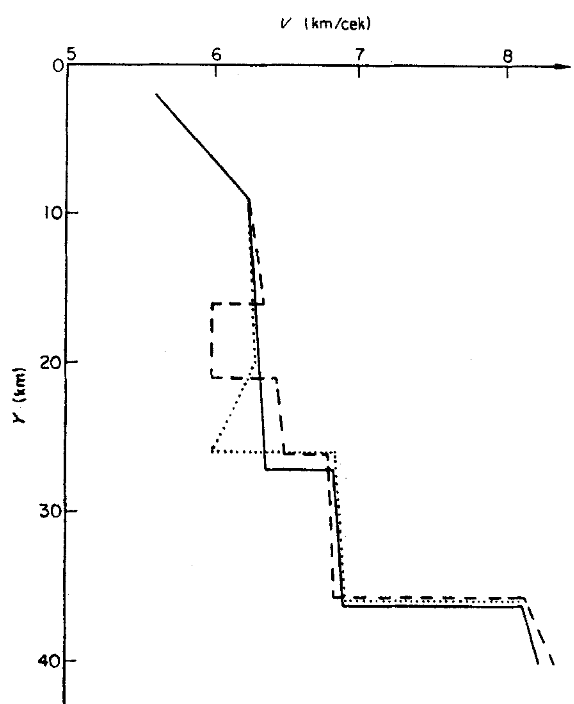

FIG. 11 Three examples of velocity-depth curves fitting the observed travel times with error less than 0·1 s.

In spite of the non-uniqueness we are able to describe some general features of all possible velocity-depth curves. In the consolidated crust, three layers are clearly separated. The upper layer has a thickness of about 7 km; it occupies the depth interval from 2–3 km to 9–10 km, depending on the thickness of unconsolidated sediments. This layer is characterized by a high velocity gradient, about 0·08–0·1 s^{-1}. The velocity of longitudinal waves in this layer increases from 5·5–5·6 km s^{-1} to 6·2–6·3 km s^{-1}.

The second layer has a thickness of 16–18 km; the velocity gradient in this layer is smaller than in the first one by a factor of about 10—it is about 0·01 s^{-1}. The velocity in this layer outside the low velocity zones lies in the range 6·3–6·5 km s^{-1}. Low velocity zones are possible here, but we are able to determine neither their depth nor the distribution of velocities inside them. The two layers mentioned above are separated by a boundary of second order (discontinuous velocity gradient with continuous velocity).

At a depth of about 25–28 km, the velocity increases sharply from 6·4–6·5 km s^{-1} to 6·8–6·9 km s^{-1}. Below this depth the third layer, with thickness 8–10 km, is situated. The velocity in this layer increases slowly, reaching 6·9–7·0 km s^{-1} at the lower boundary of the crust. The depth of this boundary is about 35–37 km. Below it the velocity jumps to a value of about 8·1 km s^{-1}.

The results obtained are in good agreement with the already known data on the structure of the crust in this region, and contribute important corrections and additions to these data.

The basic advantage of the method of inversion described here is its reliability and independence of a great number of subjective assumptions. To specify the velocity-depth distribution inside the limits which are determined here, we must use additional data.

Acknowledgments

We are grateful to Professor V. I. Keilis-Borok for his invariable attention to our work, and to Professor E. A. Flinn for fruitful discussions and patient help in editing.

Institute of Physics of the Earth,
Academy of Sciences of the USSR,
Moscow, USSR

References

Backus, G. & Gilbert, F., 1970. Uniqueness in the inversion of inaccurate gross earth data, *Phil. Trans. R. Soc. Lond.*, **A266,** 123–192.

Bessonova, E. N., Fishman, V. M. & Sitnikova, G. A., 1970. Determination of the limits for velocity distributions from discrete travel time observations: paper presented at the *Seventh Upper Mantle Symposium on Geophysical Theory and Computers*, Södergarn, Sweden.

Gerver, M. & Markushevitch, V., 1966. Determination of seismic wave velocity from the travel-time curve, *Geophys. J. R. astr. Soc.*, **11,** 165–173.

Gerver, M. & Markushevitch, V., 1967. On the characteristic properties of travel-time curves, *Geophys. J. R. astr. Soc.*, **13,** 241–246.

Ince, E. L., 1956. *Ordinary differential equations*, Dover Publications, Inc., New York.

Johnson, L. E. & Gilbert, F., 1972a. Inversion and inference for teleseismic ray data: in *Methods in computational physics*, vol. 12, Seismology: Body Waves and Sources, eds. B. Alder *et al.*, Academic Press, Inc., New York.

Johnson, L. E. & Gilbert, F., 1972b. A new datum for use in the body wave travel time inverse problem, *Geophys. J. R. astr. Soc.*, vol. **30**, 373–380.
Keilis-Borok, V. I., 1972. The inverse problem of seismology; Proceedings of the International School of Physics ' Enrico Fermi ', Course L, *Mantle and core in planetary physics*, ed. J. Coulomb and M. Caputo, Academic Press, New York.
Knopoff, L. & Teng, T. L., 1965. Analytical calculation of the seismic travel time problem, *Revs. Geophys.*, **3**, 11–24.
Lehmann, I., 1962. Recent studies of body waves in the mantle of the Earth, *Geophys. J. R. astr. Soc.*, **3**, 288–298.
Markushevitch, V. & Reznikov, E., 1973. Determination of velocity distributions from travel time curves using given lower bounds of velocity (in Russian) *Vychislitelnaya Seismologiya*, No. 6.
McMechan, G. A. & Wiggins, R. A., 1972. Depth limits in body wave inversion, *Geophys. J. R. astr. Soc.*, in press.
Ryaboyi, V. A., 1966a. The structure of the crust and upper mantle along a deep seismic sounding profile from Kipet-Dag to the Aral Sea (in Russian): *Sovietskaya Geologiya*, No. 5, 159–162.
Ryaboyi, V. A., 1966b. Kinematic and dynamic features of the wave connected with discontinuities in the crust and mantle (in Russian): *Izv. Akad. Nauk SSSR, Ser. Geofiz.*, No. 3, 74–82.
Valus, V., 1968. Determination of seismic structures from a set of observations (in Russian): *Vychislitelnaya Seismologiya*, No. 4, 3–15.
Wiggins, R. A., McMechan, G. A. & Toksöz, M. N., 1973. The range of earth structure nonuniqueness implied by body wave observations, *Revs. Geophys. Space Phys.*, **11**, 87–114.
Yanovskaya, T. B., 1962. Computation of velocity-depth curves for the upper mantle in Europe considered as an inverse mathematical problem: *Veroffentlichungen des Instituts für Bodendynamik und Erdbebenforschung in Jena*, Heft 77.
Yanovskaya, T. B. & Asbel, I. Y., 1964. The determination of velocity in the upper mantle from observations of *P* waves, *Geophys. J. R. astr. Soc.*, **8**, 274–278.

Appendix

Properties of Clairaut's equation

Clairaut's equation is a first-order linear differential equation of the form:

$$y = xy' + \phi(y') \tag{A1}$$

where ϕ is a given function (see, for example, Ince (1956)). The general solution is the one-parameter family of straight lines

$$y = Cx + \phi(C). \tag{A2}$$

Under the condition $\phi'(p) \neq 0$, the singular solution is (in parametric form):

$$x = -\phi'(y'),\ y = -y'\phi'(y') + \phi(y') \tag{A3}$$

which is an envelope of the family (A2). Suppose we have a travel-time curve $T(X)$, and consider the Clairaut equation

$$y(p) = py' + T(-y'). \tag{A4}$$

We take a point of the travel-time curve $T_i = T(X_i)$, and let $p_i = (dT/dX)|_{T_i(X_i)}$. The straight line $y_i(p) = T_i - pX_i$ is a tangent to the curve $\tau(p)$ at the point $[p_i, \tau(p_i)]$. We have $y_i(p_i) = T_i - p_i X_i = \tau(p_i)$ and $y_i'(p) = -X_i = -X(p_i) = \tau'(p_i)$. The function $y_i(p)$ is a solution of (A4), and each $y_i(p)$ is a tangent of the curve $\tau(p)$. Therefore $\tau(p)$ is an envelope of the family of curves $\{y_i(p)\}$ and a singular solution of (A4).

These elementary considerations are important for understanding the method described in this paper. They allow us to construct the envelope of $\tau(p)$ from the $T_i(X_i)$ without differentiating the travel-time curve or making array measurements of the ray parameter p.